Available online at www.sciencedirect.com
ScienceDirect
Journal of Hazardous Materials 157 (2008) 432–440
Journal of Hazardous Materials
www.elsevier.com/locate/jhazmat

Immobilization of aqueous Hg(II) by mackinawite (FeS)

Jianrong Liu [a], Kalliat T. Valsaraj [a,*], Istvan Devai [b], R.D. DeLaune [b]

[a] *Department of Chemical Engineering, Louisiana State University, Baton Rouge, LA 70803, United States*
[b] *Wetland Biogeochemistry Institute, Department of Oceanography and Sciences, School of the Coast and Environment, Louisiana State University, Baton Rouge, LA 70803, United States*

Received 22 October 2007; received in revised form 3 January 2008; accepted 3 January 2008
Available online 11 January 2008

Abstract

As one of the major constituents of acid volatile sulfide (AVS) in anoxic sediments, mackinawite (FeS) is known for its ability to scavenge trace metals. The interaction between aqueous Hg(II) (added as $HgCl_2$) and synthetic FeS was studied via batch sorption experiments conducted under anaerobic conditions. Due to the release of H^+ during formation of hydrolyzed Hg(II) species which is more reactive than Hg^{2+} in surface adsorption, the equilibrium pH decreased with the increase in Hg(II)/FeS molar ratio. Counteracting the loss of FeS solids at lower pH, the maximum capacity for FeS to remove aqueous Hg(II) was approximately 0.75 mol Hg(II) $(\text{mol FeS})^{-1}$. The comparison of X-ray power diffraction (XRPD) patterns of synthetic FeS sorbent before and after sorption showed that the major products formed from the interaction between FeS and the aqueous Hg(II) were metacinnabar, cinnabar, and mercury iron sulfides. With the addition of FeS at 0.4 g L^{-1} to a 1 mM Hg(II) solution with an initial pH of 5.6, Fe^{2+} release was approximately 0.77 mol Fe^{2+} per mol Hg(II) removed, suggesting that 77% of Hg(II) was removed via precipitation reaction under these conditions, with 23% of Hg(II) removed by adsorption. Aeration does not cause significant release of Hg(II) into the water phase.

Keywords: Sorption capacity; Mercury; Iron sulfide; pH; Interaction mechanism

1. Introduction

Bottom sediment represents one of the major reservoirs of mercury, which is a persistent pollutant in the environment. The transformation of mercury to monomethylmercury (MeHg) largely occurs in anaerobic sediments mediated by sulfate-reducing bacteria [1,2] or iron-reducing bacteria [3–5]. Studies have shown MeHg can accumulate in the aquatic food web and consumption of fish and shellfish contaminated with MeHg is the primary route of human exposure to mercury [6]. Effective remediation of mercury-contaminated sediments to reduce the release of mercury to overlying water columns is essential to minimize the contamination of fish and shellfish with MeHg. As one of the remediation methods, in situ capping can be an effective means to reduce the releases of mercury and MeHg into the water column. In situ capping is the process of placing a layer of isolating material between the contaminated sediments and the overlying water. Conventional capping materials include sand, clean sediment and other materials [7].

Depth profiles in sediments show that MeHg production occurs most actively in the surface layer of sediments. Considering the rates of mercury methylation is higher in the surface sediments, a layer of active capping material with a methylation inhibitor as the active component placed over the contaminated sediments beneath a layer of conventional sand cap should effectively reduce the MeHg production and release to the water column.

A negative correlation between MeHg in sediments and sulfides in pore water has been observed [8,9], which suggests that sulfides limit production and accumulation of MeHg in the system. Iron sulfides are one of the major sinks of mercury in sediments because of its affinity for mercury [10]. Previous studies have shown naturally occurring sulfides are excellent sorbents for aqueous solutions of Hg(II) and Hg^0 [11].

Based on the inhibition effects of sulfides on mercury methylation and the affinity of sulfides for mercury, the placement of a layer of iron sulfides over the contaminated sediments should effectively reduce releases of both mercury and MeHg. Though

* Corresponding author. Tel.: +1 225 578 6522; fax: +1 512 578 1476.
E-mail addresses: jliu7@lsu.edu (J. Liu), valsaraj@lsu.edu (K.T. Valsaraj), idevai@lsu.edu (I. Devai), rdelaun@lsu.edu (R.D. DeLaune).

0304-3894/$ – see front matter © 2008 Elsevier B.V. All rights reserved.
doi:10.1016/j.jhazmat.2008.01.006

many other factors should be considered and investigated before practical application, iron sulfides should be good candidates as components of an active capping material.

There are a variety of binary compounds formed from iron and sulfur. The common forms existing in anoxic sediments include mackinawite (FeS), greigite (Fe_3S_4), pyrite (FeS_2) and pyrrhotite ($Fe_{1-x}S$). Greigite and pyrrhotite have been shown to contain mixed Fe(II) and Fe(III) valence states [12,13], formed from the oxidation of mackinawite. Pyrrhotite is an excellent scavenger for aqueous Hg(II) complexes [14] and so is pyrite [15,16]. Mackinawite together with greigite has been accepted to be the major mineral constituents of acid volatile sulfide (AVS) in anoxic sediments and is involved in the formation of more stable pyrite [17,18]. The composition of mackinawite is not well constrained. From previous reported analyses, synthetic mackinawite has a chemical composition varying from $Fe_{0.87}S$ to $Fe_{1.15}S$ [19–21]. Presently available evidence suggests that it closely approximates stoichiometric FeS in composition [22]. In this study mackinawite will nominally be written as FeS.

FeS has a high adsorptive capacity for various divalent metals [23–27], but in-depth studies of Hg(II) sorption to FeS are rare. Metals whose sulfide phases are less soluble than FeS exhibit an increasing surface affinity with decreasing solubility [27]. At 25 °C and low to moderate ionic strength, the solubility constant for FeS is about −3.6 [28], and it is −45.7 and −45.1 for metacinnabar and cinnabar, respectively [29]. This explains the affinity of mercury to FeS.

This study was designed to test the potential of synthetic FeS to immobilize mercury in batch sorption experiments. This paper reports the results of our investigation of the immobilization of Hg(II) (added as $HgCl_2$) with FeS in aqueous solutions, including effects of the pH of both initial Hg(II) solution and equilibrium suspension on sorption, mechanism of interactions between Hg(II) and FeS, and the stability of immobilized mercury regarding oxidation.

2. Materials and methods

Chemicals used in this work were analytical grade or plus. Deionized water was produced from a Corning Mega Purification System (15.0 MΩ). Glassware and Teflon tubes were soaked in 4 M HCl for at least 24 h before rinsing with DI water and drying for use.

2.1. Preparation of FeS

Because FeS, especially wet FeS, is very reactive to oxidation, the preparation of the reactant solutions, the reaction and filtration were conducted under N_2. FeS was prepared from $FeSO_4{\cdot}(NH_4)_2(SO_4)_2{\cdot}6H_2O$ (Mohr's salt) and $Na_2S{\cdot}9H_2O$ at room temperature (24 °C). Mohr's salt is the preferred reagent with aqueous iron(II) since it is relatively resistant to oxidation [30]. After purged with high purity N_2 for half an hour, 100 ml 0.4 M Mohr's salt prepared in a separation flask was purged into 100 ml 0.4 M $Na_2S{\cdot}9H_2O$ in a three necks flask and magnetically stirred for 5 min. The suspension was then purged in the vacuum filtration system and filtered through a 0.45 μm filter. In order to remove retained ions from FeS, wet FeS was rinsed with deionized water following the procedure: immediately after filtration, the wet FeS was placed in a HDPE tube and stored in a freezer. Once the wet FeS was frozen, it was put back in the cleaned reaction flask filled with 250 ml deionized water previously purged with N_2 and stirred for 10 min under N_2, followed by filtration. The filtration process of FeS slurry was much faster after frozen and usually done within a few minutes, which helped to minimize the oxidation of FeS. The procedure was repeated three times before FeS was dried under N_2 flow. The dried FeS was placed in 1.5 ml vials and preserved under N_2 flow in a 500 ml flask.

2.2. Characterization of FeS

The specific surface area of N_2-dried FeS was measured following the multipoint N_2-BET adsorption method (Autosorb-1, Quantachrome). Approximately 1.2 g samples were loaded in the sample holder and degassed for 12 h at 100 °C under 0.035 mmHg. Scanning Electron Microprobe (SEM) (Jeol 840A) was used to obtain SEM images of the laboratory prepared FeS sorbent. In order to obtain clear images, the sample was pretreated with pure Au dust for better conductivity. The major components of the synthetic material before and after sorption were identified by X-ray power diffraction (XRPD) spectra, obtained using a Bruker/Siemens D5000 automated powder X-ray diffractometer with Cu Kα radiation.

2.3. Experimental design and procedure

A 5 mM Hg(II) stock solution was prepared by dissolving $HgCl_2$ (99.9995%, Alfa Aesar) in 32 mM HNO_3 solution (trace metal grade concentrated HNO_3 dissolved in deionized water). This stock solution was stored in a PTFE bottle for later experiments. Except for the experiments to test the capacity of FeS to retain mercury, a final concentration of 0.4 g L^{-1} of FeS was applied. The pH of the initial mercury solutions before FeS addition was adjusted to 5.6 with the exception of experiments determining pH effects on mercury retention. The sorption vessels were sealed with a rubber stopper containing inlet and outlet holes. N_2 was maintained in the head space of the vessels during the experiments in order to maintain anaerobic conditions.

For the dynamic experiments used to determine retention rates, samples were retrieved in specific time intervals. Samples were filtered through 0.45 μm PTFE syringe filters (Whatman) in order to minimize the delay between sampling and separation. Filtration was completed within 30 s after sampling.

The equilibrium experiments were conducted using either 50 ml glass centrifuge tubes or 500 ml glass flasks depending on the required volumes of relative experiments. Hg(II) solutions of designated concentrations were prepared by diluting the 5 mM stock solution with deionized water, and pH of the solutions was adjusted using 0.2 M NaOH. After purging for half an hour to exclude oxygen from the system, FeS was added into the solution. Magnetic stirring by a PTFE stirrer bar was used to maintain the homogeneity of the suspension. After 24 h, the suspension was filtered via a glass vacuum filtration unit

using 0.45 μm nitrocellulose membrane (Fisher Science). No significant adsorption of mercury to the membrane was detected.

The aeration experiments were conducted following a procedure similar to that of the equilibrium experiments during the first 24 h. After purging for 24 h with N_2, the purge gas was switched to compressed air with an approximate flow rate of 50 ml min^{-1}.

2.4. Analytical methods

All filtrates were preserved with concentrated HNO_3 to pH less than 2 before analyzing for mercury. Because HgS is completely soluble in aqua regia [31], the retained solid samples from the filtration were digested together with the filter membrane in 10 ml aqua regia (2.5 ml concentrated HCl mixed with 7.5 ml HNO_3). No mercury was detected from the digested blank filter membrane. The recovery of Hg by this method was 98 ± 2.6% (n = 14). After settling within 48 h, both the retained solid and the membrane itself were dissolved completely without any visible suspension. The oxidized mercury was reduced to volatile elemental form by addition of stannous chloride and quantitatively measured by cold vapor atomic absorption spectrometry (CVAAS) (Mercury Instruments, LabAnalyzer 254). The qualitative analysis was performed using a 7-point calibration curve ranging from 0 to 1.2 μg L^{-1}, a stable and accurate calibration was obtained ($R^2 \geq 0.999$).

pH was measured using a combination electrode (Sensorex) coupled to a pH meter (Jenco Model 60). Analysis of total iron in filtrates was performed using ICP-MS (Perkin-Elmer Sciex, Elan 9000).

FeS was estimated using the method for AVS measurement. FeS was converted to H_2S by adding 20 ml 6 M HCl to 15 ml suspension mixed with 85 ml deionized water to produce a final HCl concentration of 1 M [32]. The evolved H_2S was purged from the sample and trapped in an anti-oxidation buffer followed by measurement using a sulfide ion selective electrode (Oakton) [33].

3. Results and discussion

3.1. Properties of FeS

The freshly prepared FeS was black in color. The specific surface area of the dried FeS measured by N_2-BET method was 7.8 m^2 g^{-1}. The measured specific surface area of mackinawite varies broadly (7–47 m^2 g^{-1}) [34] as determined by the N_2-BET method. Fig. 1 shows the SEM image of the N_2-dried FeS particles. The mackinawite in Fig. 1B fits the description as noted by others [24]. Previous studies [22] have demonstrated that the primary FeS precipitate formed from the reaction between Fe(II) and S(-II) in aqueous solutions at ambient temperatures and pressures is nanoparticulate stoichiometric mackinawite, $Fe_{1.00\pm0.01}S$, thus the prepared FeS should be mackinawite. This was confirmed by the XRPD pattern of the synthetic FeS shown in Fig. 7 for comparison with the pattern of the sample after sorption of Hg(II).

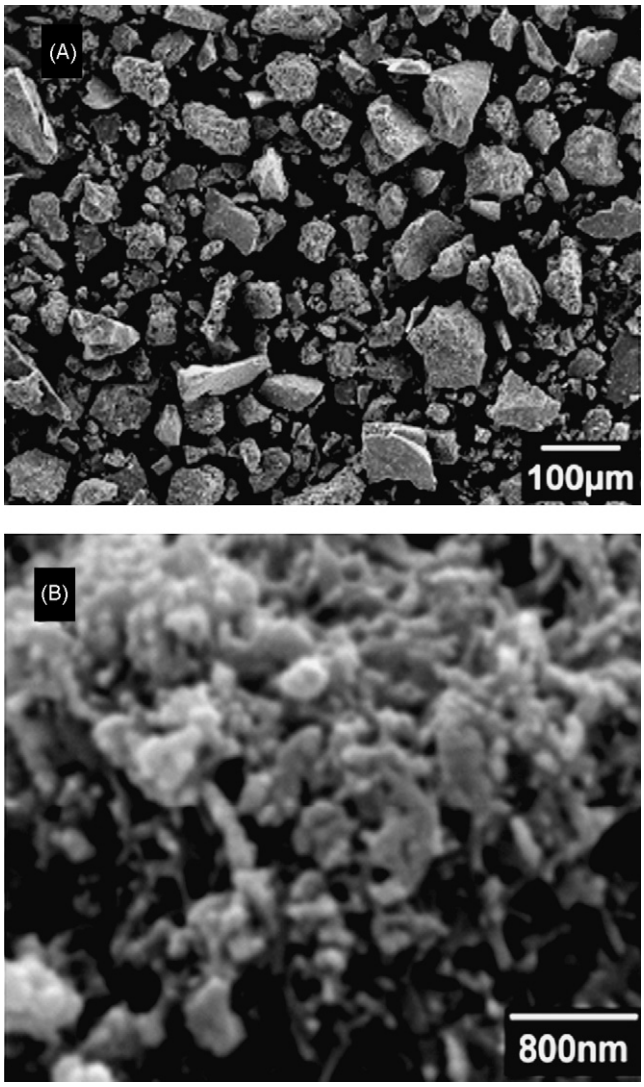

Fig. 1. Images of laboratory prepared FeS by a JEOL 840A scanning electron microscope obtained at (A) 150× magnification and (B) 30,000× magnification.

3.2. Dynamic sorption

These experiments were designed to investigate the sorption rate of Hg(II) onto the synthetic FeS and help determine the time for the sorption process to reach an approximate equilibrium. For these experiments, 0.4 g L^{-1} FeS and Hg(II) solution with an initial pH 5.6 was applied. From Fig. 2, within 3 min after FeS addition, more than a half of the initial Hg(II) was removed from the aqueous phase, with 99.99% Hg(II) removed within 20 min. This confirmed that a period of 24 h should be sufficient for the suspension to reach equilibrium. Based on this observation, a period of 24 h was chosen for the following equilibrium experiments.

3.3. Initial, equilibrium pH and Hg(II) immobilization

When 0.4 g L^{-1} (4.55 mM L^{-1}) FeS was added to a 1 mM Hg(II) solution, the Hg(II) loaded to FeS was 0.22 mol (mol FeS)$^{-1}$. Fig. 3(a) shows the relation between the initial

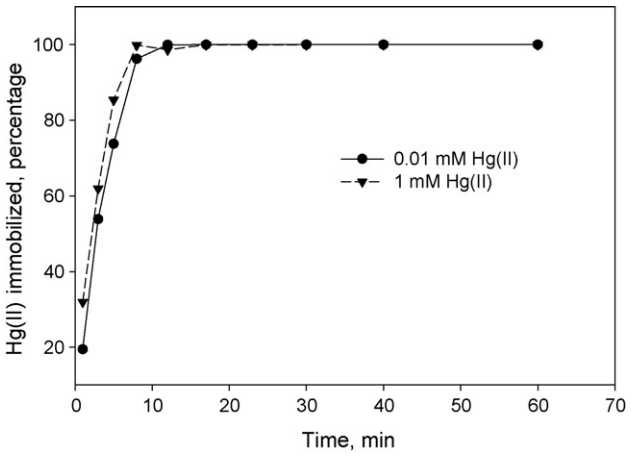

Fig. 2. Dynamic Hg(II) sorption by FeS (added FeS 0.4 g L^{-1} and initial pH of Hg(II) solutions 5.6). The legends on the figure represent the initial Hg(II) concentrations before FeS addition.

pH of solutions before FeS addition and the equilibrium pH of the suspensions 24 h after FeS addition, for 0.01, 0.1 and 1 mM initial Hg(II) concentrations, respectively. Although the equilibrium pH increased with increase in initial pH of the Hg(II) solutions, the relationship was not proportional. When the initial pH increased from 3 to 8, the equilibrium pH increases approximately from 6 to 7. When the equilibrium pH exceeded 7, the data tended to be linear. This phenomenon can be explained by the dissolution of FeS. The solubility of FeS is described by a pH-dependent reaction and a pH-independent reaction. The pH-dependent dissolution reaction can be represented by $FeS + 2H^+ \rightleftharpoons Fe^{2+} + H_2S$, with $\log Ksp^* = -3.6$ [28]. The pH-independent dissolution reaction involves the formation of the aqueous FeS cluster complex and can be represented by $FeS \rightleftharpoons FeS^0$ with $\log K_0(FeS) = -5.7$ [35].

Under acidic conditions, it is predominantly a pH-dependent reaction. The dissolution of FeS consumes hydrogen ions thus increases the pH of the suspension, which explains the "pH buffering effect" of FeS at lower initial pH as shown in Fig. 3(a). Under alkaline conditions, it becomes a pH-independent dissolution and the solubility of FeS is much lower than its solubility under acidic conditions. Thus the equilibrium pH tends to be proportional to the initial pH. The overall tendency is that FeS solubility decreases with increasing pH. Fig. 3(c) shows the relation between unreacted FeS and suspension pH, which was obtained by modeling using MINTEQA2. The equilibrium constant used for mackinawite was 3.6 and the reaction between FeS and Hg(II) was assumed via precipitation for cases when Hg(II) was present. When Hg(II)/Fe $\leq$ 0.22, no significant loss of FeS from dissolution would occur if the initial pH of Hg(II) solutions is close to neutral.

Under acidic conditions, solubility of FeS increased rapidly with decrease in pH of the suspension. When the initial pH was around 2.5 (equilibrium pH < 5), apparent loss of FeS was observed in the suspensions. This is consistent with the modeling results shown in Fig. 3(c). Because of the loss of FeS from dissolution under low pH as expected, the sorption of Hg(II) decreased (Fig. 3(b)). Further experiments with lower initial pH were not performed due to significant loss of FeS particles. When equilibrium pH > 5.5, mercury in the aqueous phase increased with equilibrium pH. The same relationship was observed for experiments with initial mercury concentrations of 0.01, 0.1 and 1 mM. It appeared that, at the same equilib-

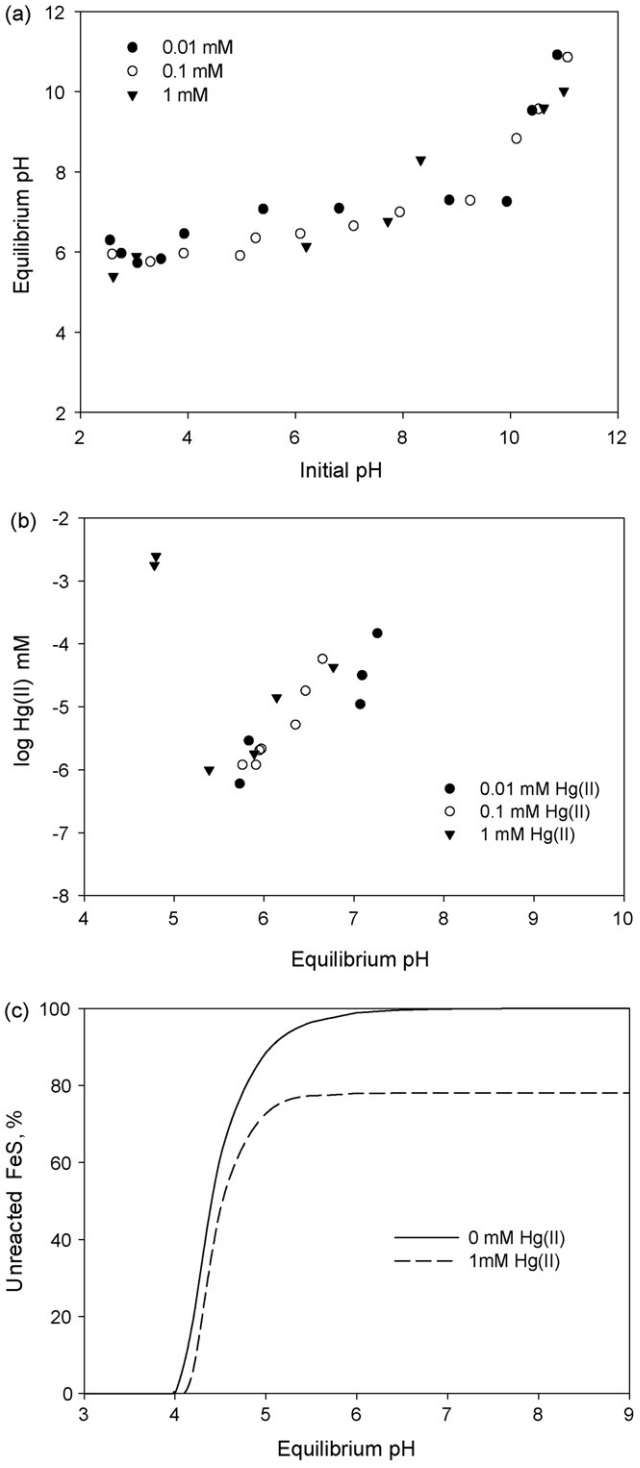

Fig. 3. pH and the immobilization of Hg(II). FeS added 0.4 g L^{-1}. (a) Relation between equilibrium pH, 24 h after FeS addition, and initial pH of Hg(II) solution before FeS addition; (b) effects of equilibrium pH on dissolved Hg(II) concentrations; (c) modeling results of unreacted FeS solids in the suspension vs. equilibrium pH.

rium pH, the mercury concentration in the aqueous phase was not apparently related to the initial concentration in the solution and the amount of mercury removed in the concentration range investigated. This was likely due to the increased dissolution of FeS nanoparticles at higher pH. It was observed that FeS was better dispersed and the suspension became darker with increase in pH. When the equilibrium pH was greater than 7.2, colorless filtrates was not obtained when filtered through a 0.45 μm membrane filter. The filtrates became darker with increase in pH, suggesting that more FeS passed through the membrane.

The slight increase of dissolved Hg(II) may also be explained by surface adsorption. It is generally assumed that the $HgOH^+$ ions are much more reactive than Hg^{2+} [14,36]. With increasing pH, the surface potential of FeS decreases, becoming less positive or more negative. The point of zero surface charge for FeS lies at pH ~7.5 [37]. It is easier for positively charged $HgOH^+$ to react with negative surfaces. However, the concentration of $HgOH^+$ decreases with increasing pH due to the formation of $Hg(OH)_2$ [38]. The effects of the decreasing surface potential and of decreasing concentration of $HgOH^+$ ions oppose each other, so that only small effects of pH on adsorption would be expected [39]. This is consistent with our experimental results.

3.4. Maximum capacity of FeS for immobilization of Hg(II)

Capacity of FeS for immobilizing Hg(II) was tested by changing added FeS concentrations with fixed initial Hg(II) concentration (1 mM) and also by changing Hg(II) concentrations with fixed initial FeS concentration (0.4 g L^{-1}). For both cases, initial pH of Hg(II) solutions was adjusted to 5.6 before FeS addition. For the case with initial Hg(II) concentration fixed at 1 mM (Fig. 4(a)), when the added FeS was in the range of 0.4–0.28 g L^{-1}, close to 100% of Hg(II) was removed from solution, with Hg(II) concentrations in filtrates less than 1.9 nM. When added FeS decreased from 0.24 to 0.16 g L^{-1}, Hg(II) removal decreased only marginally. Further decrease of added FeS in the suspension resulted in significant decrease in the percent removal of Hg(II). Although the maximum immobilization capacity reached 0.72 mol Hg(II) (mol FeS)$^{-1}$ when added FeS was as low as 0.08 g L^{-1} (loaded mole ratio Hg(II)/FeS = 1.1), only 66% of initial Hg(II) was removed. For the case with initial FeS fixed at 0.4 g L^{-1} (Fig. 5(a)), Hg(II) removed was proportional to the initial Hg(II) concentrations until a maximum capacity 0.75 mol Hg(II) (mol FeS)$^{-1}$ was reached at initial Hg(II) concentration 3.5 mM. At this maximum value, the mole ratio of loaded Hg(II)/FeS was 0.77 and the Hg(II) removed was 98.3%. From Figs. 4 and 5, the overall tendency observed was that pH decreased with the increased Hg(II)/FeS mole ratio. When Hg(II)/FeS ~0.22 (mole ratio), the equilibrium pH was near the initial pH 5.6. Decrease in pH has also been observed for sorption of Pb^{2+} and Cd^{2+} onto FeS [24]. It is hard to explain the pH decrease by simple precipitation reaction alone, because neither OH^- nor H^+ is involved in this reaction. The pH decrease should be largely caused by the surface adsorption. As stated earlier, it is usually assumed that the

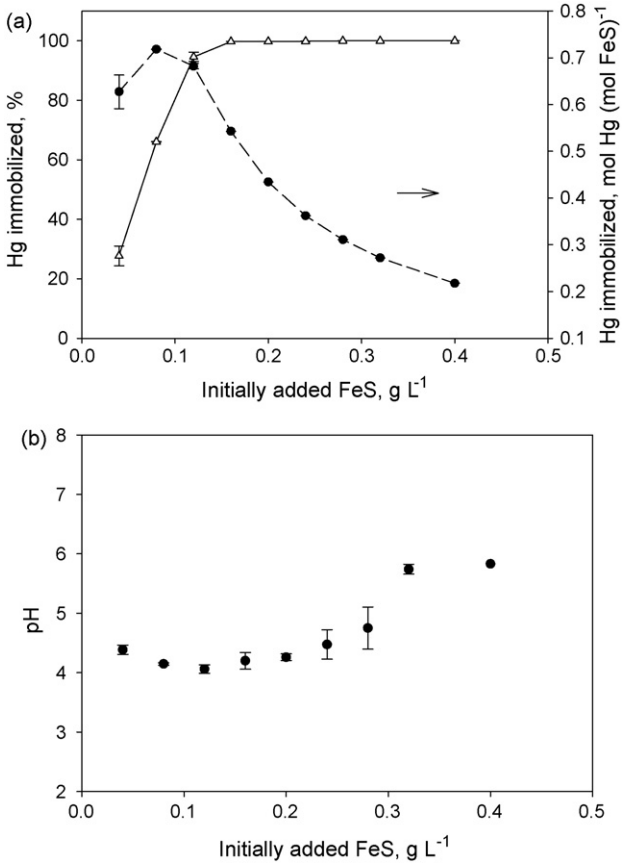

Fig. 4. Sorption of Hg(II) in suspensions with different FeS concentrations (initial Hg(II) 1 mM at pH 5.6). (a) Removed Hg(II) vs. initial FeS concentrations; (b) equilibrium pH vs. initial FeS concentrations.

charged and hydrolyzed Hg(II) species are much more reactive than Hg^{2+} [14,36]. A surface adsorption model (Eq. (1)) [36,40] explains the pH decrease prompted by the interaction between hydrolyzed Hg(II) species and mineral surface. Below pH ~7.5 [37]

$$M_{aq}^{n+} + mH_2O \rightleftharpoons M(OH)_m^{(n-m)+} + mH^+$$
$$\overline{S} + M(OH)_m^{(n-m)+} \rightleftharpoons \overline{S}M(OH)_m^{(n-m)+}$$

the positively charged FeS surface attracts OH^- ions and could be an explanation to the decrease of suspension pH.

3.5. Hg(II) immobilization and Fe^{2+} release

The precipitation reaction can be expressed as $FeS + xHg^{2+} \rightleftharpoons xFe^{2+} + (Hg_xFe_{1-x})S$ $(0 < x \leq 1)$. When $x = 1$, the ion replacement by Hg^{2+} from FeS solids is complete and HgS is formed; when $x < 1$, Fe(II) in FeS solids is partially replaced by Hg^{2+} and (Hg,Fe)S is formed. For the ion exchange reaction, equal moles of Fe^{2+} ions are released with the removal of Hg^{2+} ions. Based on this, by measuring the released Fe^{2+} in the solution, the portion of Hg(II) immobilized via ion exchange can be determined if no significant Fe^{2+} is released by dissolution. For these experiments, with loaded Hg(II)/FeS ≤ 0.22 at initial pH 5.6, it has been shown that the final pH was close to neutral (Fig. 3). This was confirmed by

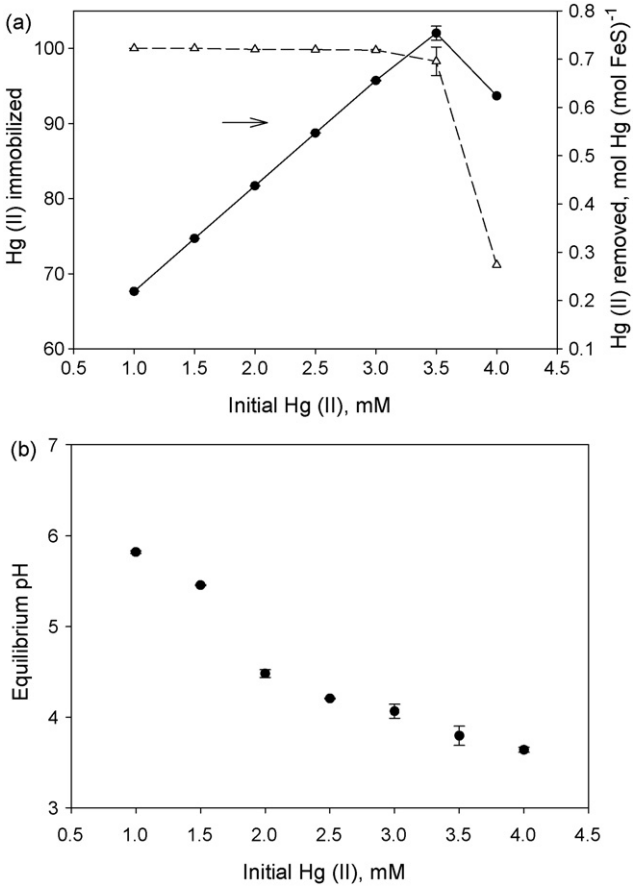

Fig. 5. Sorption of Hg(II) in suspensions with different initial Hg(II) concentrations (FeS added 0.4 g L^{-1} at initial pH 5.6). (a) Removed Hg(II) vs. initial Hg(II) concentrations; (b) equilibrium pH vs. initial Hg(II) concentrations.

the measured pH of the suspension (Fig. 6). The pH varied from 6.9 to 5.8 when the initial Hg(II) increased from 0.01 to 1 mM. Under these conditions, no significant dissolution of FeS occurs, which is especially true when initial Hg(II) is near 1 mM (Fig. 3(c)). The curves for 0.01 and 0.1 mM initial Hg(II) (which are not shown) should lie between the two curves shown

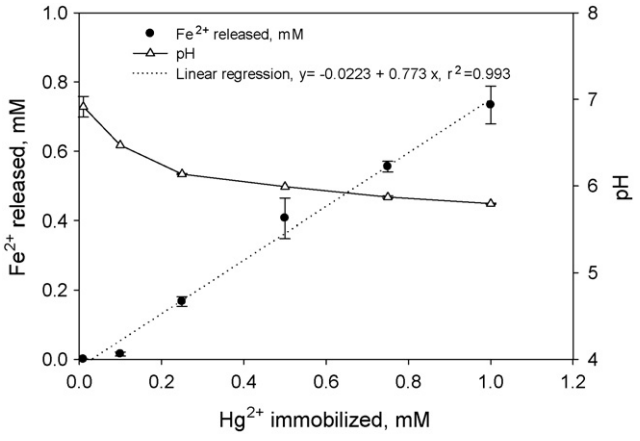

Fig. 6. Iron releases with different initial concentrations of Hg(II) (added FeS 0.4 g L^{-1} at initial pH 5.6). Under these experimental conditions, close to 100% of added Hg(II) is removed from the aqueous phase.

Table 1
Percentage of major dissolved iron species

pH	Fe^{2+} (%)	$Fe(HS)_2aq$ (%)	$Fe(OH)^+$ (%)
4	98.48	1.51	
4.5	97.31	2.43	
5	97.52	2.45	
5.5	97.59	2.50	0.01
6	97.40	2.66	0.04
6.5	96.96	3.12	0.12
7	95.43	4.28	0.38
7.5	92.54	5.91	1.16
8	89.40	6.98	3.55

in Fig. 3c and very close to the curve without the presence of Hg(II). Iron speciation shows that Fe^{2+} accounts for more than 95% of total dissolved iron (Table 1) for pH from 5.8 to 6.9. The measured total dissolved S(II) concentration was around 30 μM under the experimental conditions and was used to obtain the speciation data (Table 1) using MINTEQA2. Based on the modeling results for dissolution of FeS (Fig. 3(c)) and speciation of iron, total iron concentrations in the filtrates represent the approximate Fe^{2+} concentrations released by the ion exchange reaction between Hg(II) and FeS.

A linear relation was observed (Fig. 6) between equilibrium molar Fe^{2+} concentrations in the filtrate and molar Hg(II) concentrations was removed. It should be noted that with loaded Hg(II)/FeS $\leq$ 0.22 at initial pH 5.6, approximately 100% Hg(II) was removed from the aqueous phase (Fig. 2). The slope of the linear regression was 0.773 with an intercept of −0.0223, which meant that under the experimental conditions, approximately 77% of the Hg(II) was immobilized via ion exchange and 23% of the Hg(II) was immobilized by adsorption. Fig. 6 also showed that the pH decreased with increasing initial Hg(II) concentrations, which is consistent with the observation shown in Fig. 5 but with smaller Hg(II)/FeS loadings.

3.6. XRPD analysis

The XRPD patterns A and B shown in Fig. 7 are for the N_2-dried FeS and 'FeS' from the sorption experiments, respectively. The major components in the samples were identified with the assistance of the XRD pattern processing software (MDI Jade version 6.1) loaded with ICDD database. It was concluded that because of the nanoparticulate nature of FeS, XRPD methods routinely used to examine FeS give no pattern or show a broad peak at 5 Å (17.6° 2θ) [41]. Consistent with this conclusion, the observed XRPD pattern (Fig. 7A) of the synthetic FeS shows broad peaks with very low intensities. The broad peaks around 17.6° 2θ are indicative of FeS, with intensities and positions in reasonable agreement with peaks previously reported in the conventional XRPD pattern for FeS [34].

In contrast to pattern A in Fig. 7, peaks appear in pattern B which indicates the formation of mercury sulfides, including mercury-iron sulfide. The positions of major peaks of mercury sulfide complexes in pattern B are marked with 1 for

metacinnabar (HgS, ICDD 06-0261), 2 for mercury-iron sulfide and 3 for cinnabar (HgS, ICDD 06-0256). The highest intensity peak of cinnabar occurs at around 31.2° 2θ. The formula for mercury-iron sulfide is given as $(Hg_{0.89}Fe_{0.11})S$ (ICDD 50-1151) in the ICDD database and is referred to as (Hg,Fe)S in this paper, because it may not be the only form of mercury-iron sulfide existing in the sample. The pattern for (Hg,Fe)S is very similar to that for metacinnabar. For the major peaks with high intensities, peaks of (Hg,Fe)S overlap those of HgS and are separated slightly at the top with those for (Hg,Fe)S on the right side.

3.7. Oxidation and Hg(II) retention

In the presence of water, FeS is oxidized to FeOOH via reaction $FeS + H_2O + O_2 \rightleftharpoons FeOOH + S^0$ and S^0 can be further oxidized to sulfate [42]. After 24 h of aeration, no FeS was detected by the measurement method for AVS, which meant FeS had been completely oxidized.

From Fig. 8, we concluded that only a small amount of Hg was released into the water phase after switching the purge gas from N_2 to air, but compared to the amount retained on the solid phase it was negligible. There was no significant loss of Hg from the solid phase during 160 h of aeration. For metacinnabar and cinnabar, aeration of the suspension does not cause mercury releases from the two compounds. For Hg(II) adsorbed on FeS solid, if FeS was oxidized according to the reaction above, it should be released from FeS which would result in a significant increase in Hg concentration in the water phase. Such an increase of Hg in the water phase was not observed. This was probably due to the formation of FeOOH during oxidation and released Hg(II) was adsorbed onto FeOOH after its release from FeS. Studies [39,43–48] have shown that FeOOH itself is a good adsorbent for Hg(II).

After complete oxidation of synthetic FeS, FeOOH was separated by filtration and dried at 65 °C. The measured specific area of FeOOH (N_2-BET) was 44.7 $m^2\ g^{-1}$, which was greater than the measured specific area of FeS (7.8 $m^2\ g^{-1}$). However, its ability to immobilize Hg(II) was smaller than FeS which was not surprising because Hg(II) was removed by adsorption onto FeOOH. With the addition of 0.4 g L^{-1} FeOOH into 0.1 mM Hg(II) solution at pH 5.6, the capacity for FeOOH was 0.0044 Hg(II)/FeOOH (mole ratio). The loaded mole ratio was 0.022 and 0.22 Hg(II)/FeS for 0.1 mM and 1 mM Hg(II) solutions for the two cases in Fig. 8. Considering close to 100% of Hg(II) was immobilized and only 23% by adsorption, the portion retained by adsorption was about 0.0051 and 0.051 mol Hg(II) (mol loaded FeS)$^{-1}$ for 0.1 mM and 1 mM Hg(II) solutions, respectively. Thus we can conclude that it is possible for FeOOH to adsorb the Hg(II) released from FeS in 0.1 mM case, but it only accounts for about 10% of total Hg(II) retained by adsorption in the 1 mM case. In this case, it is impossible for FeOOH to adsorb all of the Hg(II) released from FeS after its oxidation.

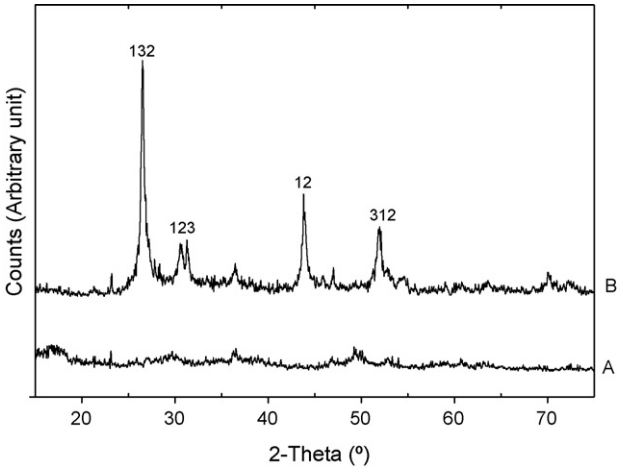

Fig. 7. XRPD patters for N_2-dried (A) fresh FeS and (B) 'FeS' after sorption (added FeS 0.4 g L^{-1} at initial pH 5.6). Numbers on the graph are used to mark the approximate peak positions of major components of the samples. 1: metacinnabar (HgS); 2: mercury iron sulfide; 3: cinnabar (HgS).

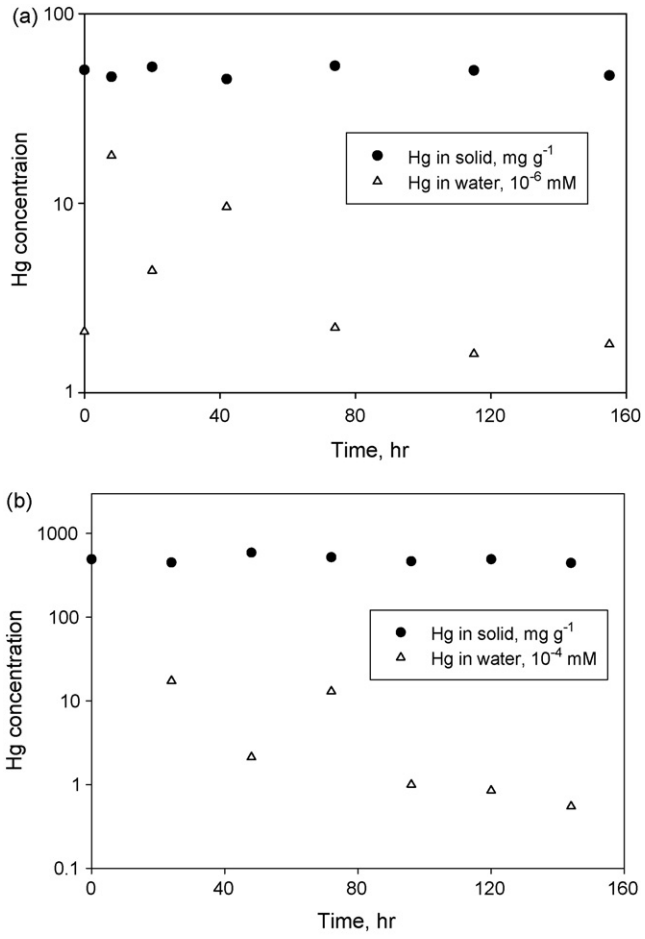

Fig. 8. Hg concentrations in suspended solid and water during aeration (added FeS 0.4 g L^{-1} and initial pH of solutions 5.6). At time '0', the purge gas was switched to air from N_2. (a) Initial Hg(II) 0.1 mM; (b) initial Hg(II) 1 mM.

HgS can adsorb Hg(II) in acidic solutions. A capacity of 1.84 mmol Hg(II) (mol HgS)$^{-1}$ has been detected in 1 mM HCl solution [49]. In less acidic solution, more Hg(II) could be adsorbed per mole of HgS. Under such condition, HgS can be another source for adsorption of released Hg(II). Another possibility is the adsorption of Hg(II) onto (Hg,Fe)S. (Hg,Fe)S should be more resistant to oxidation than FeS especially after some of

its active sites on the surface are covered by adsorbed Hg(II) complexes.

4. Conclusion

At low initial pH of Hg(II) solutions under low to moderate Hg(II) loadings, Hg(II)/FeS (mol ratio) ≤ 0.22, equilibrium pH increases by consuming H^+ via dissolution of FeS. As long as there is no significant loss of FeS by dissolution, the effects of pH on immobilization of Hg(II) are very small. With higher Hg(II)/FeS loadings, even at a neutral initial pH, the equilibrium pH decreases because less unreacted FeS is present to neutralize H^+ released by hydrolysis of Hg(II) which is promoted by adsorption.

Because of the low solubility of mercury sulfides compared to FeS, FeS has a great affinity to remove Hg(II) from solution. Although sorption process of Hg(II) to FeS includes both precipitation and adsorption, the primary mechanism for FeS to immobilize Hg(II) is via precipitation, which accounts about 77% of total Hg(II) immobilized.

Because FeS is very reactive to oxygen, steps should be taken to stabilize FeS before it can be applied as a component of an active capping material. Once Hg(II) is removed, no significant mercury will be released into the water when the system is exposed to oxidizing conditions. Oxidation product FeOOH, precipitation products HgS and (Hg,Fe)S of FeS might be the most important mechanism for the retention of released Hg(II) after the oxidation of FeS.

Acknowledgements

The authors thank Dr. Xiaogang Xie and Ms. Wanda Leblanc in the Department of Geophysics of Louisiana State University for SEM and XRPD analysis, respectively.

References

[1] C.C. Gilmour, E.A. Henry, R. Mitchell, Sulfate stimulation of mercury methylation in freshwater sediments, Environ. Sci. Technol. 26 (1992) 2281–2287.
[2] G. Compeau, R. Bartha, Methylation and demethylation of mercury under controlled redox, pH, and salinity conditions, Appl. Environ. Microbiol. 48 (1984) 1203–1207.
[3] E.J. Fleming, E.E. Mack, P.G. Green, D.C. Nelson, Mercury methylation from unexpected sources: molybdate-inhibited freshwater sediments and an iron-reducing bacterium, Appl. Environ. Microbiol. 72 (2006) 457–464.
[4] E.J. Kerin, C.C. Gilmour, E. Roden, M.T. Suzuki, J.D. Coates, R.P. Mason, Mercury methylation by dissimilatory iron-reducing bacteria, Appl. Environ. Microbiol. 72 (2006) 7919–7921.
[5] K.A. Warner, E.E. Roden, J.C. Bonzongo, Microbial mercury transformation in anoxic freshwater sediments under iron-reducing and other electron-accepting conditions, Environ. Sci. Technol. 37 (2003) 2159–2165.
[6] B. Wheatley, S. Paradis, Exposure of Canadian aboriginal people to methylmercury, Water Air Soil Pollut. 80 (1995) 3–11.
[7] M.R. Palermo, Design considerations for in situ capping of contaminated sediments, Water Sci. Technol. 37 (1998) 315–321.
[8] J.M. Benoit, C.C. Gilmour, R.P. Mason, G.S. Riedel, G.F. Riedel, Behavior of mercury in the Patuxent River estuary, Biogeochemistry 40 (1998) 249–265.
[9] J.M. Benoit, C.C. Gilmour, R.P. Mason, A. Heyes, Sulfide controls on mercury speciation and bioavailability to methylating bacteria in sediment pore waters, Environ. Sci. Technol. 33 (1999) 951–957.
[10] S. Wolfenden, J.M. Charnock, J. Hilton, F.R. Livens, D.J. Vaughan, Sulfide species as a sink for mercury in lake sediments, Environ. Sci. Technol. 39 (2005) 6644–6648.
[11] J.R. Brown, G.M. Bancroft, W.S. Fyfe, R.A.N. Mclean, Mercury removal from water by iron sulfide minerals. An electron spectroscopy for chemical analysis (ESCA) study, Environ. Sci. Technol. 13 (1979) 1142–1144.
[12] D.J. Vaughan, J.A. Tossell, Electronic structure of thiospinel minerals—results from Mo calculations, Am. Mineral. 66 (1981) 1250–1253.
[13] A.R. Pratt, I.J. Muir, H.W. Nesbitt, X-ray photoelectron and auger-electron spectroscopic studies of pyrrhotite and mechanism of air oxidation, Geochim. Cosmochim. Acta 58 (1994) 827–841.
[14] G.E. Jean, G.M. Bancroft, Heavy metal adsorption by sulfide mineral surfaces, Geochim. Cosmochim. Acta 50 (1986) 1455–1463.
[15] J.J. Ehrhardt, P. Behra, P. Bonnissel-Gissinger, M. Alnot, XPS study of the sorption of Hg(II) onto pyrite FeS_2, Surf. Interface Anal. 30 (2000) 269–272.
[16] P. Behra, P. Bonnissel-Gissinger, M. Alnot, R. Revel, J.J. Ehrhardt, XPS and XAS study of the sorption of Hg(II) onto pyrite, Langmuir 17 (2001) 3970–3979.
[17] R.A. Berner, Sedimentary pyrite formation, Am. J. Sci. 268 (1970) 1–23.
[18] D.E. Canfield, R. Raiswell, S. Bottrell, The reactivity of sedimentary iron minerals toward sulfide, Am. J. Sci. 292 (1992) 659–683.
[19] A.R. Lennie, S.A.T. Redfern, P.E. Champness, C.P. Stoddart, P.F. Schofield, D.J. Vaughan, Transformation of mackinawite to greigite: an in situ X-ray powder diffraction and transmission electron microscope study, Am. Mineral. 82 (1997) 302–309.
[20] R.A. Berner, Iron sulfides formed from aqueous solution at low temperatures and atmospheric pressure, J. Geol. 72 (1964) 293–306.
[21] R.E. Sweeney, I.R. Kaplan, Pyrite framboid formation—laboratory synthesis and marine sediments, Econ. Geol. 68 (1973) 618–634.
[22] D. Rickard, A. Griffith, A. Oldroyd, I.B. Butler, E. Lopez-Capel, D.A.C. Manning, D.C. Apperley, The composition of nanoparticulate mackinawite, tetragonal iron(II) monosulfide, Chem. Geol. 235 (2006) 286–298.
[23] M.J. Wharton, B. Atkins, J.M. Charnock, F.R. Livens, R.A.D. Pattrick, D. Collison, An X-ray absorption spectroscopy study of the coprecipitation of Tc and Re with mackinawite (FeS), Appl. Geochem. 15 (2000) 347–354.
[24] C.A. Coles, S.R. Rao, R.N. Yong, Lead and cadmium interactions with mackinawite: retention mechanisms and the role of pH, Environ. Sci. Technol. 34 (2000) 996–1000.
[25] T. Arakaki, J.W. Morse, Coprecipitation and adsorption of Mn(II) with mackinawite (FeS) under conditions similar to those found in anoxic sediments, Geochim. Cosmochim. Acta 57 (1993) 9–14.
[26] J.W. Morse, G.W. Luther, Chemical influences on trace metal sulfide interactions in anoxic sediments, Geochim. Cosmochim. Acta 63 (1999) 3373–3378.
[27] J.W. Morse, T. Arakaki, Adsorption and coprecipitation of divalent metals with mackinawite (FeS), Geochim. Cosmochim. Acta 57 (1993) 3635–3640.
[28] W. Davison, The solubility of iron sulfides in synthetic and natural waters at ambient temperature, Aquat. Sci. 53 (1991) 309–329.
[29] D. Dyrssen, K. Kremling, Increasing hydrogen sulfide concentration and trace metal behavior in the anoxic baltic waters, Mar. Chem. 30 (1990) 193–204.
[30] D. Rickard, Kinetics of FeS precipitation. 1. Competing reaction mechanisms, Geochim. Cosmochim. Acta 59 (1995) 4367–4379.
[31] N. Mikac, D. Foucher, S. Niessen, J.C. Fischer, Extractability of HgS (cinnabar and metacinnabar) by hydrochloric acid, Anal. Bioanal. Chem. 374 (2002) 1028–1033.
[32] H.E. Allen, G.M. Fu, B.L. Deng, Analysis of acid volatile sulfide (AVS) and simultaneously extracted metals (SEM) for the estimation of potential toxicity in aquatic sediments, Environ. Toxicol. Chem. 12 (1993) 1441–1453.
[33] H. Brouwer, T.P. Murphy, Diffusion method for the determination of acid-volatile sulfides (AVS) in sediment, Environ. Toxicol. Chem. 13 (1994) 1273–1275.

[34] M. Wolthers, S.J. Van der Gaast, D. Rickard, The structure of disordered mackinawite, Am. Mineral. 88 (2003) 2007–2015.
[35] D. Rickard, The solubility of FeS, Geochim. Cosmochim. Acta 70 (2006) 5779–5789.
[36] Mg. Macnaugh, R.O. James, Adsorption of aqueous mercury (II) complexes at oxide–water interface, J. Colloid Interface Sci. 47 (1974) 431–440.
[37] M. Wolthers, L. Charlet, P.R. Van der Linde, D. Rickard, C.H. Van der Weijden, Surface chemistry of disordered mackinawite (FeS), Geochim. Cosmochim. Acta 69 (2005) 3469–3481.
[38] E. Schuster, The behavior of mercury in the soil with special emphasis on complexation and adsorption processes—a review of the literature, Water Air Soil Pollut. 56 (1991) 667–680.
[39] N.J. Barrow, V.C. Cox, The effects of pH and chloride concentration on mercury sorption. 1. By goethite, J. Soil. Sci. 43 (1992) 295–304.
[40] R.O. James, T.W. Healy, Adsorption of hydrolyzable metal ions at oxide–water interface. 1. Co(II) adsorption on SiO_2 and TiO_2 as model systems, J. Colloid Interface Sci. 40 (1972) 42–52.
[41] D. Rickard, J.W. Morse, Acid volatile sulfide (AVS), Mar. Chem. 97 (2005) 141–197.
[42] E.D. Burton, R.T. Bush, L.A. Sullivan, Acid-volatile sulfide oxidation in coastal flood plain drains: iron–sulfur cycling and effects on water quality, Environ. Sci. Technol. 40 (2006) 1217–1222.
[43] P. Bonnissel-Gissinger, M. Alnot, J.P. Lickes, J.J. Ehrhardt, P. Behra, Modeling the adsorption of mercury(II) on (hydr)oxides II: α-FeOOH (goethite) and amorphous silica, J. Colloid Interface Sci. 215 (1999) 313–322.
[44] G.E. Brown, G.A. Parks, Sorption of trace elements on mineral surfaces: modern perspectives from spectroscopic studies, and comments on sorption in the marine environment, Int. Geol. Rev. 43 (2001) 963–1073.
[45] L. Gunneriusson, S. Sjoberg, Surface complexation in the H^+-goethite (α-FeOOH)-Hg(II)-chloride system, J. Colloid Interface Sci. 156 (1993) 121–128.
[46] C.S. Kim, J.J. Rytuba, G.E. Brown, EXAFS study of mercury(II) sorption to Fe- and Al-(hydr)oxides. I. Effects of pH, J. Colloid Interface Sci. 271 (2004) 1–15.
[47] A.J. Slowey, G.E. Brown, Transformations of mercury, iron, and sulfur during the reductive dissolution of iron oxyhydroxide by sulfide, Geochim. Cosmochim. Acta 71 (2007) 877–894.
[48] N.J. Barrow, V.C. Cox, The effects of pH and chloride concentration on mercury sorption. 2. By a soil, J. Soil Sci. 43 (1992) 305–312.
[49] S.M. Hasany, M.M. Saeed, M. Ahmed, Retention of Hg(II) by solid mercury sulfide from acidic solution, Sep. Sci. Technol. 34 (1999) 487–499.